HHS Public Access

Author manuscript

*J Biophotonics*. Author manuscript; available in PMC 2018 December 01.

Published in final edited form as:

*J Biophotonics*. 2017 December ; 10(12): 1732–1742. doi:10.1002/jbio.201700004.

# Photobiomodulation leads to enhanced radiosensitivity through induction of apoptosis and autophagy in human cervical cancer cells

**Gholamreza Esmaeeli Djavid, MD, PhD**[1], **Bahareh Bigdeli, PhD**[2], **Bahram Goliaei, PhD**[2,*], **Alireza Nikoofar, MD**[3], and **Michael R Hamblin, PhD**[4,5]

[1]Medical Laser Research Center, Academic Center for Education, Culture, and Research (ACECR), Tehran, Iran

[2]Laboratory of Biophysics and Molecular Biology, Institute of Biochemistry and Biophysics (IBB), University of Tehran, Tehran, Iran

[3]Radiotherapy Department, Firoozgar Hospital, Iran University of Medical sciences. Tehran, Iran

[4]Wellman Center for Photomedicine, Massachusetts General Hospital, Boston, Massachusetts, USA

[5]Department of Dermatology, Harvard Medical School, Boston, Massachusetts, USAHarvard-MIT Division of Health Sciences and Technology, Cambridge, Massachusetts, USA

## Abstract

The radiomodulatory effect of photobiomodulation (PBM) has recently been studied in cancer cells. The aim of this study was to investigate cellular mechanisms involved in the X-ray radiosensitivity of HeLa cells pre-exposed to PBM. HeLa cells were irradiated with 685 nm laser at different energy densities prior to X-ray ionizing radiation. After irradiation, clonogenic cell survival, cell death due to apoptosis and autophagy were determined. Levels of intracellular reactive oxygen species (ROS), DNA damage and, cell cycle distribution after PBM were measured. PBM at different energy densities (5–20 J/cm$^2$) was not cytotoxic. However, HeLa cells pre-exposed to 20 J/cm$^2$ showed enhanced inhibition of colony formation following ionizing radiation. Enhanced radiosensitivity was due to increased oxidative stress, DNA damage, and radiation-induced apoptosis and autophagy. These results suggest that 685 nm PBM at a higher energy density could possibly be a promising radiosensitizing agent in cervical cancer, to decrease the radiation dose delivered, and therefore prevent the side-effects that are associated with cancer radiotherapy

### Keywords

photobiomodulation; low-level laser therapy; ionizing radiation; radiosensitization; autophagy; cervical cancer cells

**Corresponding Author:** goliaei@ut.ac.ir.

## 1. Introduction

Cervical cancer is the most common gynecological malignancy among women after endometrial and ovarian cancers [1]. Although surgery is the first line treatment for cervical cancer, it is unlikely that surgery alone will be sufficient to remove all remaining cancerous cells. Radiotherapy with ionizing radiation (IR) helps to remove any remaining neoplastic cells and has also been shown to reduce risk of recurrence [2]. The outcome of radiotherapy is not always satisfactory, since cervical cancer cells have lower sensitivity to IR compared to other cancer types [3, 4]. It is therefore important to sensitize these cells to IR, to increase the chances of successful treatment without intolerable side-effects.

Genotoxicity and DNA damage is the central lethal event in cells exposed to IR. Among them, double-strand breaks (DSBs) in DNA can damage genomic integrity leading to cell death in mammalian cells [5–7]. On the other hand, the capacity of cells to carry out DNA repair is the main determinant in sensitivity of cancer to IR. Increased DNA repair capability can lead to radioresistance. Therefore, modulation of cellular responses to IR through reducing the DNA repair capacity of cells has been a longstanding goal in radiation biology [8]. The repair of DSBs and radiation-induced apoptotic cell death are both energy-demanding processes consuming a large amount of cellular ATP [9, 10]. Therefore, regulating mitochondrial bioenergetics could alter the cellular responses to genotoxic stressors such as IR [11].

Photobiomodulation (PBM) or low-level laser irradiation (LLLI) can modulate several cellular responses [12–17]. The absorption of photons emitted from lasers or other light sources by cellular photoacceptors creates oxidative stress at a cellular level and leads to generation of a burst of intracellular reactive oxygen species (ROS) [13, 18–20]. Lower energy densities of PBM that only produce a brief burst of low-intensity ROS can stimulate beneficial processes such as proliferation, differentiation, and viability [12, 21]. On the other hand higher energy densities that produce a high level of ROS that can be prolonged can induce pro-apoptotic effects and can inhibit proliferation in vitro [15, 19, 22]. These paradoxical effects of PBM are called “biphasic dose response” and depend on the energy density of light delivered [12]. ROS homeostasis and ROS-mediated signaling have an important role in cellular response following PBM. The generated ROS by PBM even at very low energy densities can initiate redox-signaling and can activate redox-sensitive transcription factors such as the Akt/GSK3beta pathway and nuclear factor kappa B (NF-kB) [23–25]. These transcription factors stimulate anti-apoptotic and/or cell survival responses. Increasing the energy of PBM provides an ever-larger amount of ROS that may eventually reach cytotoxic levels. Cytotoxic levels of ROS cause various types of cellular damage and can induce apoptosis via inactivation of the Akt/GSK3beta signaling pathway [13, 14, 19]. Furthermore, apoptosis can be directly initiated from mitochondrial ROS generation following high energy PBM. This apoptosis results from reduction of mitochondrial membrane potential and the so-called “ROS-dependent ROS release” [13, 26].

Recently, the radiomodulatory effects of PBM have been reported in various cells especially cervical cancer cells [27–29]. However, the mechanism of the radiomodulatory effects of PBM in cervical cancer cells is still uncertain. This study aimed to investigate the cellular

responses when PBM was followed with X-ray ionizing radiation in human cervical cancer cells. Additionally, we evaluated the role of oxidative stress, DNA damage and cell cycle progression.

## 2. Materials and Methods

### 2.1. Cell line and culture conditions

Human cervix adenocarcinoma cell line HeLa was purchased from National Cell Bank of Iran (NCBI C115, Pasteur Institute, Iran). The cells were cultured in RPMI-1640 medium (Gibco-31800-089), containing 10% fetal bovine serum (Gibco-10270), 100 U/ml penicillin (Sigma, USA-PENNA) and 100 μg/ml streptomycin (Jaberebn-Hayan, Iran- 4D1751) in a humidified incubator with 5% $CO_2$ at a temperature of 37°C.

### 2.2. Photobiomodulation

The protocol of PBM was described in detail in our previous study [27]. A continuous wave 685 nm laser (BTL-5000, Prague, Czech Republic) with 50 mW output power was used for PBM. This device was specifically designed to provide uniform irradiation from beyond the wall of the culture plates on which the cells were seeded. The reduction in power density caused by this type of irradiation was calculated using a laser power meter (ThorLab PM100A, USA). Laser irradiation was applied once at 16.6 mW/cm$^2$ power density at 0 (control), 5, 10, 20 J/cm$^2$ energy densities at 0 (control), 5, 10 and 20 minutes, respectively. The area of exposure was held constant, and included the entire area of the colonies on the culture plates.

### 2.3. Mitochondrial activity assay

Mitochondrial activity was measured using the tetrazolium salt assay (MTT). HeLa cells were trypsinized and seeded at an initial density of $1\times10^4$ cells/cm$^2$ in 96 well plates. After 24 hours, the cells were irradiated with 685 nm laser light at 5, 10 and 20 J/cm$^2$ energy densities. At 48 hours after PBM, medium was removed from each well and 50 mL MTT solution (Sigma, USA-M2128) (2 mg/mL) was added. After three hours incubation, medium was removed and 100 μL dimethyl sulfoxide was added (Merck, Germany- 102952) to each well. Absorbance at 570 and 630 nm wavelengths was measured with BioTek plate reader. Difference of absorbance at the two wavelengths represented the amount of formazan produced. At 48 h post PBM mitochondrial activity can be taken as a measure of cell proliferation.

### 2.4. Clonogenic survival assay after X-ray ionizing radiation

The clonogenic assay protocol was described in our previous study [27]. Briefly, the cells were seeded into each well of 12 well-plates. Prior to X-ray radiation, the cells were irradiated with 685 nm laser at 0 (control), 5, 10 and 20 J/cm$^2$ energy densities. After a one-hour incubation, the cells were exposed to 6 MeV X-ray photons (Siemens Primus linear accelerator, Germany) at a dose rate of 200 cGy/minute. Then, cells were incubated for nine days to form colonies. The colonies were fixed in 2% formaldehyde (Sigma, USA- F8775) and stained with crystal violet (0.5%) (Sigma, USA- C3886). The survival fraction was calculated for each dose of X-ray IR (0, 2, 4, 6 Gy).

### 2.5. Apoptosis Detection and Quantification

Morphological changes due to apoptosis induced by PBM alone and the combination with X-ray radiation were detected by fluorescence microscopy (Zeiss, Germany) of cultures stained with acridine orange/ethidium bromide (AO/EB) and quantified using flow cytometry according to published procedures [30, 31]. Treated HeLa cells were pelleted, resuspended in 200 μL of PBS, and stained with AO-EB. The final concentrations of AO (Sigma, USA- A6014) and EB (Sigma, USA- E7637) were 0.1 and 0.25 mM, respectively. All samples were stained and analyzed immediately at room temperature. Flow cytometric analysis was performed on CyFlow Space (Parpec, Germany). Data were analyzed by using FloMax software.

### 2.6. Autophagy Detection

To detect the occurrence of autophagy in HeLa cells, staining of acidic vesicular organelles (AVOs) with acridine orange (Sigma, USA- A6014) was performed. Lysosome-related markers such as AVOs are used to evaluate autophagy. In acridine orange (AO)-stained cells, the cytoplasm and nucleolus fluoresce green, while acidic compartments fluoresce red. The intensity of the red fluorescence emission is proportional to the degree of acidity. Morphological changes due to autophagy induced by PBM alone and the combination with X-ray radiation were examined by fluorescence microscopy (Zeiss, Germany) of cultures stained with AO and quantified using flow cytometry. After PBM and X-ray radiation, HeLa cells were incubated for 6 hours. Then, the cells were stained with 2 μg/mL acridine orange for 15 minutes.

### 2.7. Reactive oxygen species (ROS) assay

Quantitation of ROS generated by PBM was performed by 2′,7′-dichloro-dihydrofluorescin diacetate (DCF-DA, Sigma-D6883) staining. DCF-DA passes easily through the cell membrane where it is deactylated to a non-fluorescent dihydrofluorescein, and an increase in fluorescence signal can be observed upon its oxidation. After PBM, the cells were trypsinized and plated at $2\times10^4$ cells/$cm^2$ density into 12-well plates. After 48 hours, the cells were irradiated with laser light at different energy densities. Thirty minutes later, DCF-DA was added to the medium at a final concentration of 2μM. The plates were incubated for 45 minutes in the dark (37°C, 5% $CO_2$). Then medium containing DCF-DA was removed and washed twice with PBS. The fluorescence emission of ROS can be detected by using excitation at 488 nm (blue) and emission at 530 nm (green) wavelengths. The generation of ROS was visualized and quantified using fluorescence microscopy and fluorescence plate reader (BioTek H4), respectively.

### 2.8. DNA damage assay

The single cell gel electrophoresis, commonly called the “comet assay”, is a simple and fast method for detecting DNA breaks at the single cell level. In this study, the alkaline comet assay was performed immediately after PBM. Immediately after PBM, cells were trypsinized and suspended in 70 μL low melting point agarose (Sigma, USA- A9414) (0.5% in PBS) and 65 μL of the suspension was deposited on a fully frosted slide which was pre-coated with 80 ml 1% agarose (Sigma, USA- A9539) in PBS. The agarose was allowed to

set at 4°C for 10 min. The slides were then put into a tank filled with lysis buffer solution (2.5 M NaCl (Sigma, USA- S7653), 0.1 M EDTA (Sigma, USA- 798681), 10 mM Tris (Sigma, USA- 10708976001)/HCl (Sigma, USA- H1758) adjusted to pH 10, 1% Triton X-100 (Merck, Germany- 108643) freshly added) for 1 hour at 4°C. To allow DNA unwinding, the slides were incubated in fresh electrophoresis buffer (0.3 M NaOH (Sigma, USA- S8045) and 1 mM EDTA, pH 13.6) for 30 min at 4°C. The slides were then placed into an electrophoresis tank and electrophoresis was performed at 16 V (1 V/cm, 300 mA) for 30 min at room temperature. After electrophoresis, the slides were placed in fresh neutralization buffer (0.4 M Tris/HCl adjusted to pH 7.5) before staining with 50 μl ethidium bromide solution (20 μg/ml) and were observed at 20× magnification using a fluorescence microscope (Zeiss Axoscope 2, Germany). Through a randomized process a 100 cells per slide were visually scored and analyzed using image analysis software (Tri Tek Comet Score 1.5).

### 2.9. Cell cycle assay

Cell cycle assay by quantitation of DNA content is a common method to distinguish cells in different phases of the cell cycle by flow cytometry. Approximately $1\times10^6$ HeLa cells/$cm^2$ treated with PBM were washed twice by centrifugation (200g, 5 min, 4°C) in PBS and were fixed in cold 70% ethanol (Sigma, USA- 24102). The fixed cells in ethanol were kept at least 2 hours at −20°C. Then, the cells were washed twice with cold PBS by centrifugation and the cell pellet were resuspended in 300 μL of PBS containing 100 μg/mL RNAse (SinaClon BioScience, Iran-PR891628C), 10 μg/mL propidium iodide (PI) (Sigma, USA- P4170) and, 10 ml of 0.1 % (v/v) Triton X-100 (Merck, Germany- 108643) for 15 minutes in the dark. The fluorescence emission of PI can be detected by using excitation at 488 nm (blue) and emission at >650 nm (red) wavelengths. Data were analyzed by using CyFlow Space (Parpec, Germany) and analyzed using FloMax software.

### 2.10. Statistical Analysis

Statistical analyses were performed using SPSS 17 software. Data are presented as means ± standard error of mean (SEM). For continuous variables, means were compared by one-way analysis of variance (ANOVA) and Tukey's post hoc testing. The level of statistical significance with 95% level of confidence was set at a two-tailed p-value of 0.05.

## 3. Results

### 3.1. PBM did not significantly influence the proliferation of HeLa cells

The results of proliferation of HeLa cells measured at 48 hours after PBM at different energy densities is shown in Figure 1. PBM with 685 nm wavelength at an energy density up to 20 J/$cm^2$ did not significantly affect the proliferation rate of HeLa cells.

### 3.2. PBM reduced cell survival fraction after X-ray IR in clonogenic survival assay

Table 1 shows the percentage of HeLa cells surviving after X-ray IR according to clonogenic survival assay. The cells were pre-exposed by PBM at 0 (control), 5, 10 and 20 J/$cm^2$ with 685 nm wavelength. Compared with control HeLa cells (X-ray radiation only without PBM), the survival fraction of HeLa cells treated with 4 Gy and 6 Gy doses of X-ray radiation was

significantly decreased when pre-treated with PBM at 20 J/cm$^2$ energy density. These results indicate that PBM at a higher energy density produced radiosensitization of HeLa cells and enhanced the cytotoxic response to IR in a dose-dependent manner.

### 3.3. PBM induced intracellular ROS production

Intracellular ROS production was assessed at 30 min after PBM. Florescent microscopy showed that PBM could induce intracellular ROS production in HeLa cells (Figure 2). The cells treated with PBM showed higher ROS intensity in a dose dependent manner as compared to untreated cells (Figure 3). The quantitative measurement of ROS intensity showed that PBM at 5 J/cm$^2$ energy density the ROS levels were approximately 2.4-fold higher than the control value. ROS production was increased to approximately 2.7-fold and 4.4-fold at the energy densities 10 J/cm$^2$ (images not shown) and 20 J/cm$^2$ of PBM.

### 3.4. PBM induced DNA damage in HeLa cells

We found that DNA damage was induced by PBM, as demonstrated by the alkaline comet assays. The alkaline comet assay revealed that DNA fragments migrated to form comet-like images indicative of DNA damage (Figure 4). In the control cells (untreated with PBM), high-density DNA was observed in the comet heads with smooth margins and intact nuclei. For quantifying DNA damage, Olive tail moment was calculated by the product of the amount of DNA and the mean distance of migration in the tail [32]. Compared with control HeLa cells (untreated with PBM), the mean Olive moment significantly increased more than 2.7-fold in the cells treated with 20 J/cm$^2$ PBM. (Figure 4)

### 3.5. PBM slightly increased X-ray induced apoptosis in HeLa cells

A representative fluorescent photograph of apoptotic cells is shown in Figure 6. According to flow cytometry analysis (Figure 5-a,b), PBM alone, even at a higher energy density (20 J/cm$^2$), was unable to induce apoptosis efficiently (2.8%). After 6 Gy X-ray radiation alone, the apoptotic cell fraction significantly increased (9.5% v.s. 0.9% in control cells). In HeLa cells treated with PBM, X-ray radiation was able to induce more apoptotic cell fraction (12%). However, it is likely that this increased apoptosis was due to additive contributions of the separate effects of PBM and X-ray radiation (Figure 6) rather than any synergistic combination.

### 3.6. PBM induced autophagy in HeLa cells

A representative red fluorescent micrograph of AVOs is shown in Figure 7 which indicates fluorescence microscopy of autophagy in HeLa cells after IR, and the combination of PBM followed by IR. Acridine orange images were taken at 6 hours after PBM or X-ray radiation. Increased positive cytoplasmic staining for AVOs after PBM combined with IR with suggests that autophagy could be a potential mechanism to explain the increased radiosensitivity after PBM + IR.

### 3.7. PBM did not induced cell cycle arrest

The results of cell cycle analysis of cellular DNA content in HeLa cells after PBM is shown in Figure 8. Analysis of the cell cycle profile showed that proportion of cells in different

phases of the cell cycle was not significantly altered after PBM. The cell population in G2/M phase reflects cellular proliferation. PBM did not affect HeLa cell proliferation after 685 nm PBM at different energy densities (see Figure 1).

## 4. Discussion

The aim of this study was to investigate the mechanism of how the radiosensitivity of HeLa cells was increased when the cells were pre-exposed to 685 nm PBM. The findings from this study noted that HeLa cells could indeed be sensitized to IR by pre-exposure to a higher energy density of PBM. The radiation survival fraction of HeLa cells was decreased after pre-exposing to 20 J/cm$^2$ PBM at 685 nm. We assumed that PBM at higher energy density could enhance potentially lethal damage (PDL) after IR. Increasing PDL can lead to hypersensitizing the cells to IR. Fixation of DNA damage or increasing un-repairable DNA damage is the major component of radiosensitisation. According to our hypothesis, we selected a short incubation time between PBM and IR to accumulate the PDL before disappearing acute effects of PBM.

The radiosensitizing effects of PBM at higher energy densities could be also explained by the ROS homeostasis. The cellular response and outcome will depend on the amount of ROS generation, the duration of the stress response, as well as cell type. Several studies showed that PBM causes oxidative stress and generates intracellular ROS in dose-dependent manner [33–35]. ROS is composed of highly reactive oxidizing agents that are produced as by-products from cellular metabolism under both normal and pathological conditions, and especially by cellular exposure to physical insults or chemical toxins [36]. However physiological (normal) levels of ROS play an important role in signaling pathways involved in cell proliferation and survival. When oxidative stress surpasses the capacity of cellular antioxidant systems to neutralize the oxidants, the excess ROS is able to react with almost all cellular biomolecules to induce oxidative damage to DNA, lipids and proteins. This oxidative damage will lead to the death of cells damaged beyond their repair capabilities [13]. Production of ROS which is excessively prolonged, or which is excessive in magnitude, can both constitute oxidative stress. Our finding showed that 685 nm PBM induced ROS generation in a dose-dependent manner. A clear distinction between damaging oxidative stress and beneficial redox signaling is hard to define. However, it is expected that increasing energy densities of PBM causes increasing levels of oxidative stress that gradually progress from beneficial levels to relatively damaging levels that can even reach cytotoxic levels. Oxidative stress has been shown to lead to various types of cellular damage such as DNA damage [13, 37]. DSBs due to oxidative stress can lead to cell death following ionizing radiation [8]. Increasing level of DSBs will inhibit DNA repair and enhanced fixation of damage inducing radiosensitisation. The capacity of the cells to cope with DNA damage determines cell death due after IR [38]. This can be appreciated by the fact that the level of expression of DNA damage induced proteins and DNA repair enzymes within different cells often correlates with the resistance or sensitivity of the respective cells toward IR. The alkaline comet assay indicated that 685 nm PBM delivered at energy densities above 10 J/cm$^2$ caused DNA damage (both SSBs and DSBs) more than 2-fold in comparison with background control levels. Previously, Houreld et al. (2007) reported that after 30 minutes, a single exposure of 632.8 nm PBM at 5 J/cm$^2$ caused a significant increase in DNA damage

[39]. However, it is not clear whether this DNA damage is completely repairable. The phosphorylation of the minor histone H2AX protein to form the γ-H2AX protein is necessary for the repair of DSBs [40]. The γ-H2AX molecules accumulate at sites of DSBs, which can be thereby be visualized in fluorescence microscopy. Therefore, persistence of γ-H2AX indicates impaired DNA repair. Khan et al. (2015) examined γ-H2AX after laser irradiation [41]. They did not find any evidence for non-repaired DSBs after laser irradiation. Therefore, oxidative DNA damage due to PBM in the range of common therapeutic doses is likely to be repairable, but nevertheless it may still affect cell hemeostasis and signaling.

The decrease of the survival fraction after IR in HeLa cells pre-exposed to PBM, indicates increased cell death. Therefore, it is necessary to identify which cell death pathway is enhanced when IR is delivered after PBM. To address this, we assessed the ability of pre-exposure to PBM to induce two types of programmed cell death including apoptosis (type I) and autophagy (type II) when followed by IR [42, 43]. Apoptosis is known to be the primary mechanism of cell death following IR [32]. A high level of resistance to apoptosis induced by IR is a particular feature of HeLa cells types [3, 4]. In the present study, induction of apoptosis following IR at a dose of 6 Gy was observed in up to 10% of the cells, as previously shown by Ghoari et al. (2014) PBM alone at 20 $J/cm^2$ slightly induced apoptosis but it was not significant in comparison with untreated cells [44]. The frequency of IR-induced apoptosis in HeLa cells pre-exposed to PBM slightly increased over IR alone by the same % as found for HeLa cells treated by PBM alone. Therefore, it seems that PBM and IR could increase cell death due to apoptosis additively. In contrast, we found that pre-exposing HeLa cells to PBM significantly increased autophagy as measured by AVOs after IR. Autophagy can be an indicator of accumulated intracellular stress caused by different conditions such as starvation or exposure to IR [45–47]. It seems that oxidative stress due to PBM at higher energy densities could have triggered autophagy. Finally, we can assume that induction of autophagy in HeLa cells pre-exposed to PBM is (at least partly) responsible for the increased cell death observed following IR. Therefore we suggest that PBM may sensitize HeLa cells to IR through upregulation of autophagy.

The cytotoxicity caused by IR is cell cycle dependent [48]. Cells are generally most sensitive when undergoing mitosis, and relatively radioresistant at early G1 and late S phases of the cell cycle. Moreover, cells are relatively radiosensitive in the G1/S transition and the G2/M phase [49]. The question remains whether the influence of PBM on HeLa cell cycle plays a role in the radiosensitization phenomenon. Although cells in the G0/1 phase are more sensitive to radiation than late S-phase cells, radiosensitizing effects were also observed at higher energy densities of PBM, which resulted in a blockade later in the S phase. However, the S-phase block itself can not directly explain the radiosensitization. The progression of the cell cycle is mainly governed by cyclin-dependent kinases (CDK) [50]. G1 phase progression and S-phase entry both require the activities of CDKs. Cell cycle progression is dependent on the synthesis and degradation of newly formed CDK molecules. Cell cycle arrest can occur if CDKs fail to degrade. Our finding shows that PBM could not induce cell cycle arrest while it could slightly increase cell cycle progression from G0/G1 to S phase as it has been shown previously [29]. Therefore, cell cycle arrest is not likely to be responsible for radiosensitization of HeLa cells.

It must also be considered that the limitation of the present study was that the HeLa cells received PBM and ionizing radiation in an in-vitro model which might not simulate in-vivo or a clinical situation. Although quantitative in-vitro data can be extrapolated reasonably to the in vivo situation with a good understanding of the interdependent factors and cellular mechanisms, more research utilizing different cell types and PBM parameters and both in-vivo and clinical setting is needed to support our conclusions.

## 5. Conclusion

In conclusion, the results of this study suggest that 685 nm PBM can act as a potential radiosensitizing agent for cervical cancer cells, as shown by the decreased survival fraction following IR. The increased cell death is partly by more apoptosis and to a greater extent to more autophagy occurring when IR is preceded by PBM at a higher energy density (at least 20 J/cm$^2$). These sensitizing effect of PBM at higher energy densities could also be caused by increased oxidative stress and more DNA damage. Hence, 685 nm PBM can be suggested as a promising candidate for a combination anticancer therapy to decrease the radiation dose delivered to patients with cervical cancer who are receiving radiotherapy, and therefore help to prevent the side effects that are associated with cancer radiotherapy. However, this would require future in-vivo and clinical investigation. It should also be noted that PBM used on its own, is becoming increasingly employed to reduce or mitigate the side effects of radiotherapy in cancer patients [51, 52]. The molecular mechanism(s) responsible for the radiosensitizing effect of PBM are still not completely clear. Therefore it will be necessary to conduct more research to explore the detailed mechanisms of the radiosensitizing effect of PBM. In particular, it will be interesting to investigate the effect of PBM when delivered after IR (rather than before).

## Supplementary Material

Refer to Web version on PubMed Central for supplementary material.

## Acknowledgments

Michael R Hamblin was funded by US NIH grant R01AI050875

## References

1. Franco EL, Schlecht NF, Saslow D. Cancer J. 2003; 9:348–359. [PubMed: 14690309]
2. Kim TJ, Lee JW, Song SY, Choi JJ, Choi CH, Kim BG, Lee JH, Bae DS. Br J Cancer. 2006; 94:1678–1682. [PubMed: 16721365]
3. Huang EY, Chen YF, Chen YM, Lin IH, Wang CC, Su WH, Chuang PC, Yang KD. Cell death & disease. 2012; 3:e251. [PubMed: 22237208]
4. Novak ER. Obstetrics and gynecology. 1954; 4:251–259. [PubMed: 13194251]
5. Karin M. Nature. 2006; 441:431–436. [PubMed: 16724054]
6. Paris F, Fuks Z, Kang A, Capodieci P, Juan G, Ehleiter D, Haimovitz-Friedman A, Cordon-Cardo C, Kolesnick R. Science. 2001; 293:293–297. [PubMed: 11452123]
7. Vousden KH, Prives C. Cell. 2009; 137:413–431. [PubMed: 19410540]
8. Kulkarni R, Thomas RA, Tucker JD. Environ Mol Mutagen. 2011; 52:229–237. [PubMed: 20740641]

9. Bakkenist CJ, Kastan MB. Cell. 2004; 118:9–17. [PubMed: 15242640]
10. Ward I, Chen J. Curr Top Dev Biol. 2004; 63:1–35. [PubMed: 15536012]
11. Gafter-Gvili A, Herman M, Ori Y, Korzets A, Chagnac A, Zingerman B, Rozen-Zvi B, Gafter U, Malachi T. Leuk Res. 2011; 35:219–225. [PubMed: 20619454]
12. Huang YY, Sharma SK, Carroll J, Hamblin MR. Dose Response. 2011; 9:602–618. [PubMed: 22461763]
13. Wu S, Xing D, Gao X, Chen WR. J Cell Physiol. 2009; 218:603–611. [PubMed: 19006121]
14. Huang L, Wu S, Xing D. Journal of cellular physiology. 2011; 226:588–601. [PubMed: 20683916]
15. Chu J, Wu S, Xing D. Cancer letters. 2010; 297:207–219. [PubMed: 20579806]
16. Hu WP, Wang JJ, Yu CL, Lan CC, Chen GS, Yu HS. The Journal of investigative dermatology. 2007; 127:2048–2057. [PubMed: 17446900]
17. Ben-Dov N, Shefer G, Irintchev A, Wernig A, Oron U, Halevy O. Biochimica et biophysica acta. 1999; 1448:372–380. [PubMed: 9990289]
18. Zhang J, Xing D, Gao X. Journal of cellular physiology. 2008; 217:518–528. [PubMed: 18615581]
19. Sun X, Wu S, Xing D. The FEBS journal. 2010; 277:4789–4802. [PubMed: 20977672]
20. Grossman N, Schneid N, Reuveni H, Halevy S, Lubart R. Lasers in surgery and medicine. 1998; 22:212–218. [PubMed: 9603282]
21. Sperandio FF, Simoes A, Correa L, Aranha AC, Giudice FS, Hamblin MR, Sousa SC. J Biophotonics. 2015; 8:795–803. [PubMed: 25411997]
22. Wu S, Xing D, Wang F, Chen T, Chen WR. Journal of biomedical optics. 2007; 12:064015. [PubMed: 18163831]
23. Shefer G, Barash I, Oron U, Halevy O. Biochimica et biophysica acta. 2003; 1593:131–139. [PubMed: 12581857]
24. Zhang L, Zhang Y, Xing D. Journal of cellular physiology. 2010; 224:218–228. [PubMed: 20333643]
25. Chen AC, Arany PR, Huang YY, Tomkinson EM, Sharma SK, Kharkwal GB, Saleem T, Mooney D, Yull FE, Blackwell TS, Hamblin MR. PloS one. 2011; 6:e22453. [PubMed: 21814580]
26. Zorov DB, Juhaszova M, Sollott SJ. Physiol Rev. 2014; 94:909–950. [PubMed: 24987008]
27. Djavid GE, Goliaie B, Nikoofar A. Photomed Laser Surg. 2015; 33:452–459. [PubMed: 26332916]
28. Ramos Silva C, Cabral FV, de Camargo CF, Nunez SC, Mateus Yoshimura T, de Lima Luna AC, Maria DA, Ribeiro MS. J Biophotonics. 2016; 9:1157–1166. [PubMed: 27322660]
29. Barasch A, Raber-Durlacher J, Epstein JB, Carroll J. Support Care Cancer. 2016; 24:2497–2501. [PubMed: 26670917]
30. Liegler TJ, Hyun W, Yen TS, Stites DP. Clinical and diagnostic laboratory immunology. 1995; 2:369–376. [PubMed: 7664185]
31. Ribble D, Goldstein NB, Norris DA, Shellman YG. BMC biotechnology. 2005; 5:12. [PubMed: 15885144]
32. Olive PL, Banath JP. Nat Protoc. 2006; 1:23–29. [PubMed: 17406208]
33. Callaghan GA, Riordan C, Gilmore WS, McIntyre IA, Allen JM, Hannigan BM. Lasers Surg Med. 1996; 19:201–206. [PubMed: 8887924]
34. Eichler M, Lavi R, Friedmann H, Shainberg A, Lubart R. Photomed Laser Surg. 2007; 25:170–174. [PubMed: 17603856]
35. Lavi R, Shainberg A, Friedmann H, Shneyvays V, Rickover O, Eichler M, Kaplan D, Lubart R. J Biol Chem. 2003; 278:40917–40922. [PubMed: 12851407]
36. Miura Y. J Radiat Res. 2004; 45:357–372. [PubMed: 15613781]
37. Roots R, Kraft G, Gosschalk E. Int J Radiat Oncol Biol Phys. 1985; 11:259–265. [PubMed: 2982769]
38. Rosenberg A, Knox S. Int J Radiat Oncol Biol Phys. 2006; 64:343–354. [PubMed: 16414370]
39. Houreld N, Abrahamse H. Photomed Laser Surg. 2007; 25:78–84. [PubMed: 17508841]
40. Pilch DR, Sedelnikova OA, Redon C, Celeste A, Nussenzweig A, Bonner WM. Biochem Cell Biol. 2003; 81:123–129. [PubMed: 12897845]
41. Khan I, Tang E, Arany P. Sci Rep. 2015; 5:10581. [PubMed: 26030745]

42. Eriksson D, Stigbrand T. Tumour Biol. 2010; 31:363–372. [PubMed: 20490962]
43. Panganiban RA, Snow AL, Day RM. Int J Mol Sci. 2013; 14:15931–15958. [PubMed: 23912235]
44. Ghorai A, Bhattacharyya NP, Sarma A, Ghosh U. Scientifica (Cairo). 2014; 2014:438030. [PubMed: 25018892]
45. Chaurasia M, Bhatt AN, Das A, Dwarakanath BS, Sharma K. Free Radic Res. 2016; 50:273–290. [PubMed: 26764568]
46. Gewirtz DA, Hilliker ML, Wilson EN. Radiother Oncol. 2009; 92:323–328. [PubMed: 19541381]
47. Zhuang W, Qin Z, Liang Z. Acta Biochim Biophys Sin (Shanghai). 2009; 41:341–351. [PubMed: 19430698]
48. Denekamp J. Int J Radiat Biol Relat Stud Phys Chem Med. 1986; 49:357–380. [PubMed: 3510997]
49. Gudkov AV, Komarova EA. J Clin Invest. 2010; 120:2270–2273. [PubMed: 20577043]
50. Hochegger H, Takeda S, Hunt T. Nat Rev Mol Cell Biol. 2008; 9:910–916. [PubMed: 18813291]
51. Zecha JA, Raber-Durlacher JE, Nair RG, Epstein JB, Elad S, Hamblin MR, Barasch A, Migliorati CA, Milstein DM, Genot MT, Lansaat L, van der Brink R, Arnabat-Dominguez J, van der Molen L, Jacobi I, van Diessen J, de Lange J, Smeele LE, Schubert MM, Bensadoun RJ. Support Care Cancer. 2016
52. Zecha JA, Raber-Durlacher JE, Nair RG, Epstein JB, Sonis ST, Elad S, Hamblin MR, Barasch A, Migliorati CA, Milstein DM, Genot MT, Lansaat L, van der Brink R, Arnabat-Dominguez J, van der Molen L, Jacobi I, van Diessen J, de Lange J, Smeele LE, Schubert MM, Bensadoun RJ. Support Care Cancer. 2016

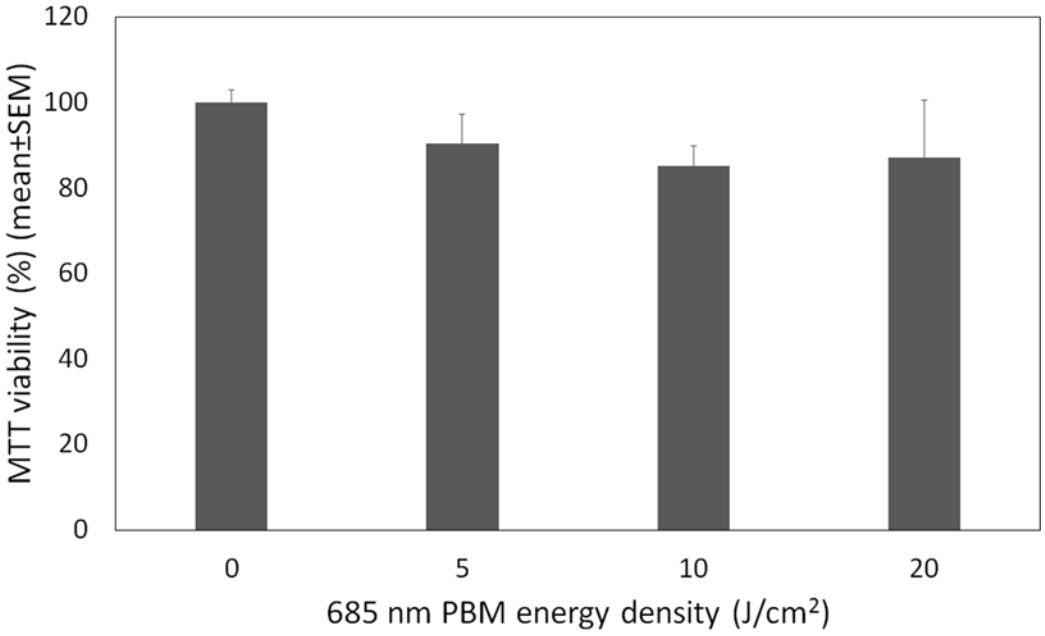


**Figure 1.**

MTT assay of HeLa cells at different energy of 685 nm PBM. The data are shown as mean ± SEM for at least three independent experiments. Statistical analysis between the groups was determined by ANOVA; *P < 0.05, compared with control cells.

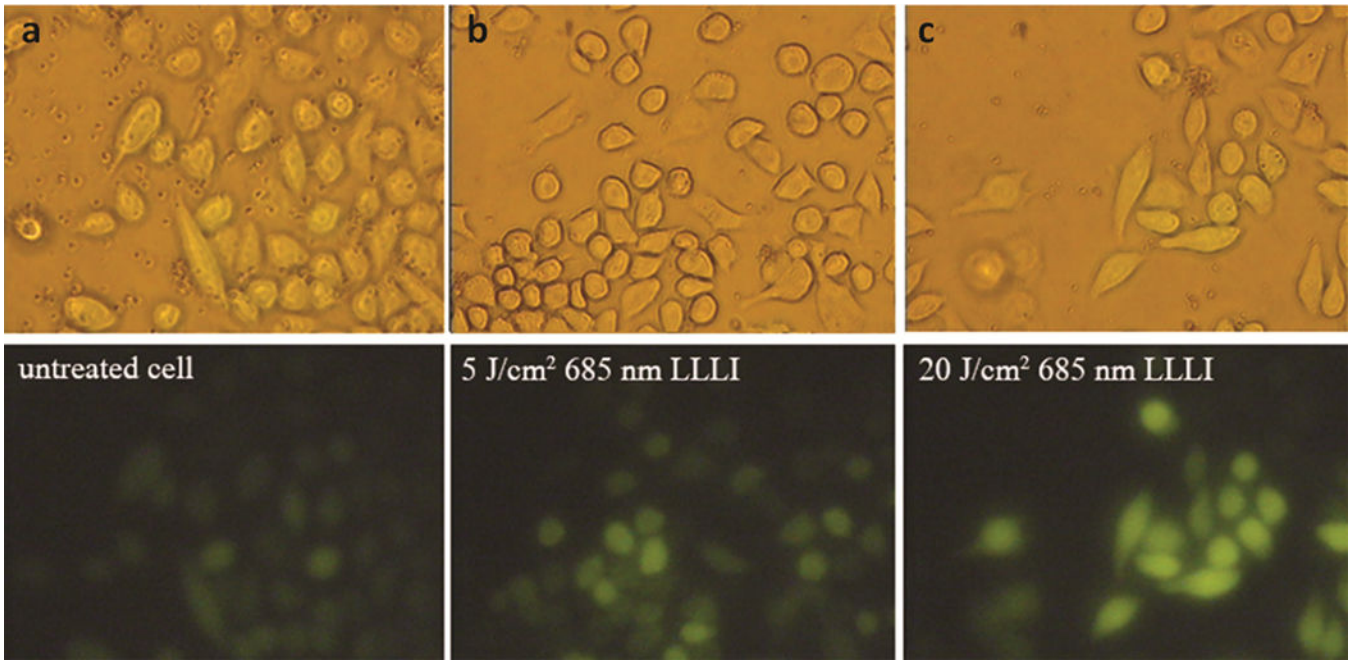


**Figure 2.**

Detection of intracellular ROS in HeLa cells treated by PBM at different energy densities after 30 minutes. Florescence invert microscopy in HeLa cells shows a green DCF florescence in HeLa cells treated by 685 nm PBM in a dose-dependent manner.

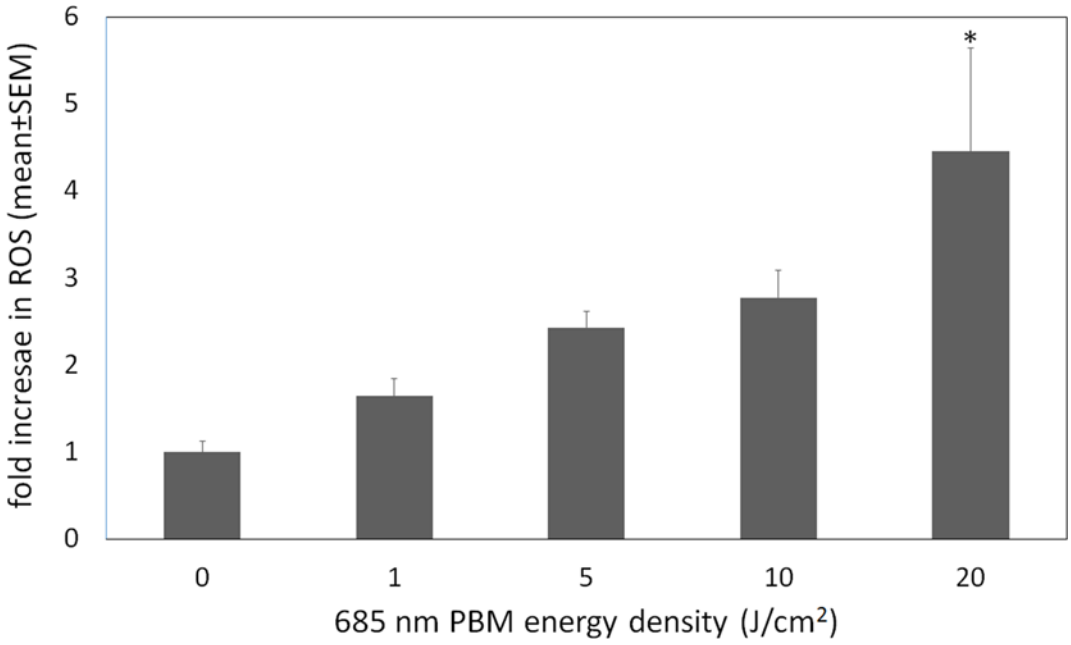


**Figure 3.**

Detection of intracellular ROS in HeLa cells. DCF fluorescence signal was monitored at Excitation/Emission 490/525 nm with bottom read mode using plate reader BioTek H4. Intracellular ROS production was sustained increasingly to approximately 2.7-fold and 4.4-fold at the dose densities 10 J/cm$^2$ and 20 J/cm$^2$ of PBM. The data are shown as mean ± SEM for at least three independent experiments. Statistical analysis between the groups was determined by ANOVA; *P < 0.05, compared with control cells.

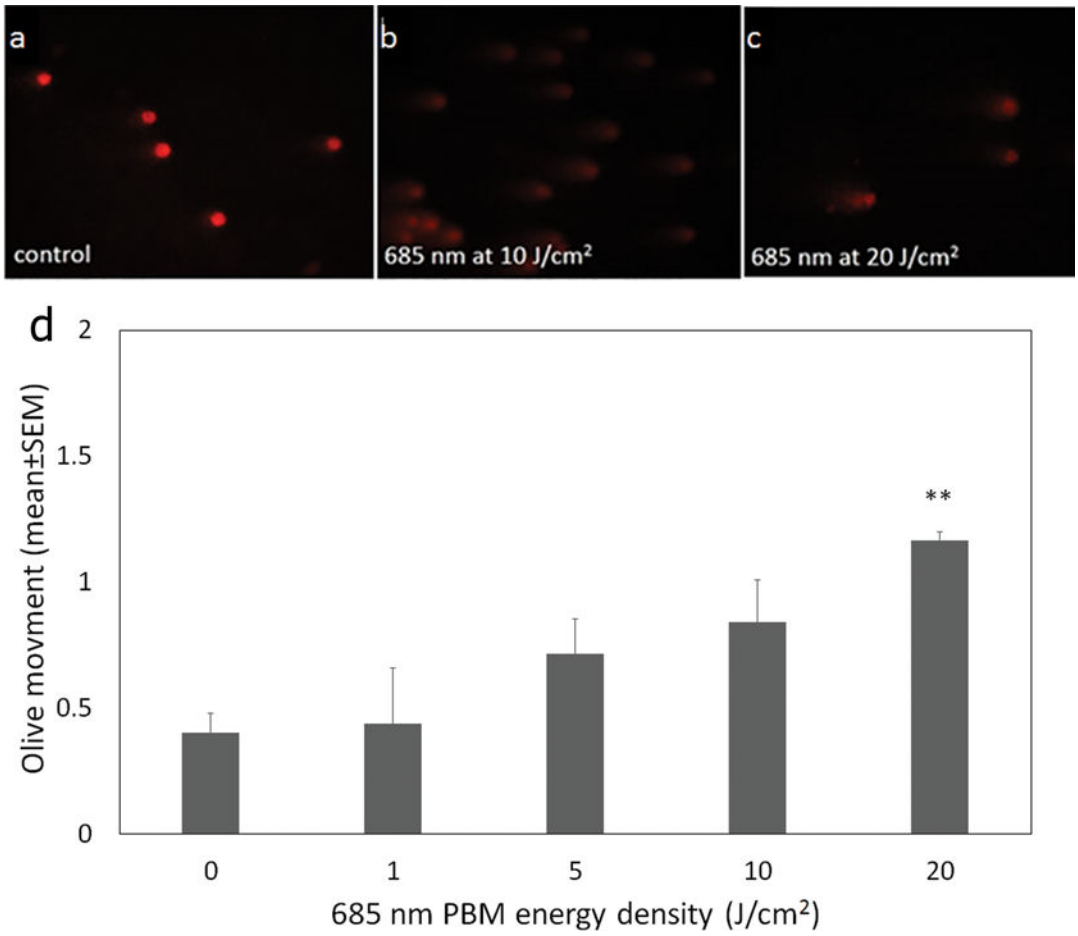


**Figure 4.**

Comet assay images after DNA-staining with ethidium bromide after PBM at different energy densities. Estimation of DNA damage following PBM, by the olive tail moment measurements from alkaline comet assays. Olive movement was sustained increasingly according to energy densities. In the cells treated with 20 J/cm$^2$ PBM, the DNA comets exhibited broom-shaped tails (Figure 4-c). The percentages of comet-positive HeLa cells increased at 20 J/cm$^2$ energy density compared with the control (Figure 4-d). The data are shown as mean ± SEM for at least three independent experiments. Statistical analysis between the groups was determined by ANOVA; **P < 0.01, compared with non-irradiated cells.

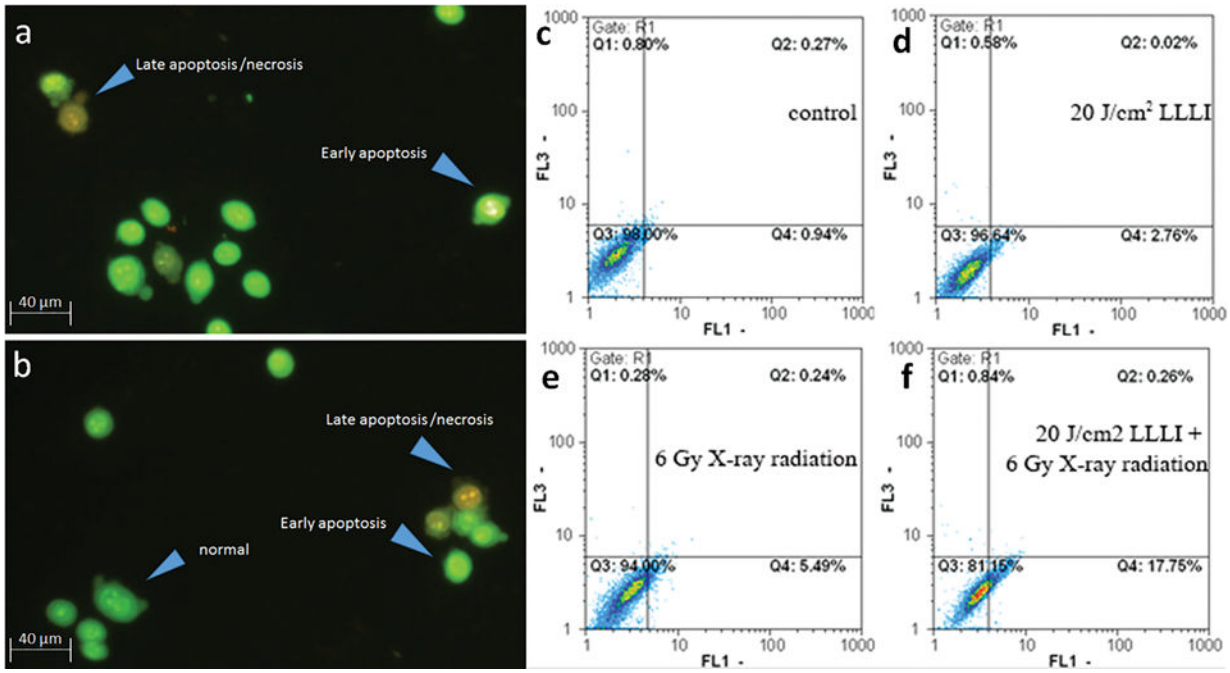


**Figure 5.**

Florescence microscopy characteristics of apoptosis in HeLa cells (Figure 6-a,b). AO/EB double staining of HeLa cells shows normal cells are uniformly green, early apoptotic cells are green with bright green dots in their nuclei as a consequence of chromatin condensation and nuclear fragmentation. Late apoptotic cells/necrosis are orange. Figure 6-c–f shows flow cytometry output on cells were treated by PBM at 20 J/cm2 and 6 Gy dose of X-ray radiation. After 6 hours incubation, cells were stained with acridine orange and ethidium bromide and the intensity of the red and green fluorescence was measured by flow cytometry in FL1-H and FL3-H channel, respectively.

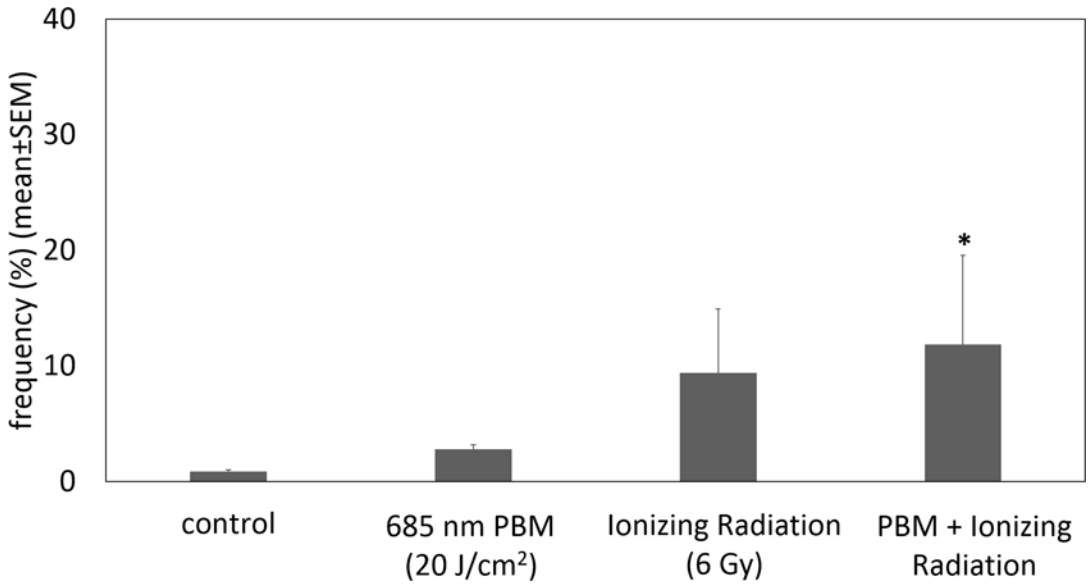


**Figure 6.**

Frequency of apoptotic HeLa cell following PBM and ionizing radiation. The data are shown as mean ± SEM for at least three independent experiments. Statistical analysis between the groups was determined by ANOVA; *P < 0.05, compared with non-irradiated cells to PBM.

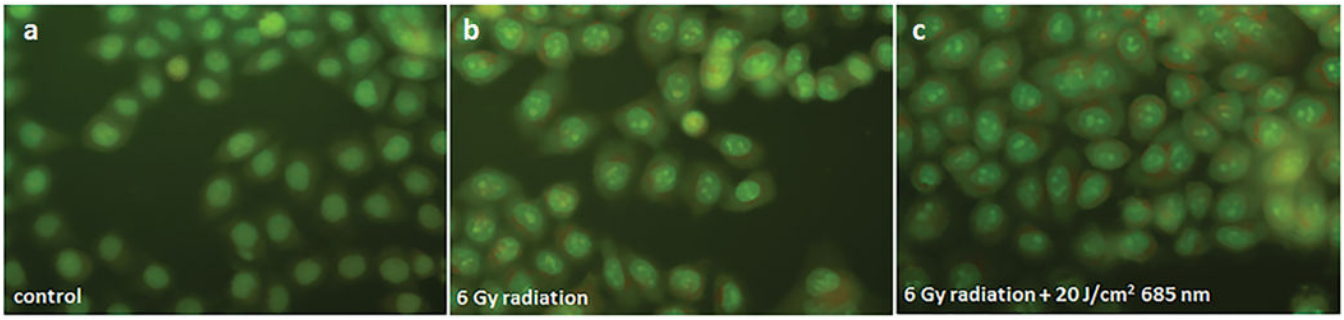


**Figure 7.**

Florescence microscopy characteristics of autophagy in HeLa cells. Acridine orange images were taken at 6 hours after PBM or X-ray radiation. The HeLa cells with positive staining for AVOs was measured using flow cytometry 6 hours after treatment.

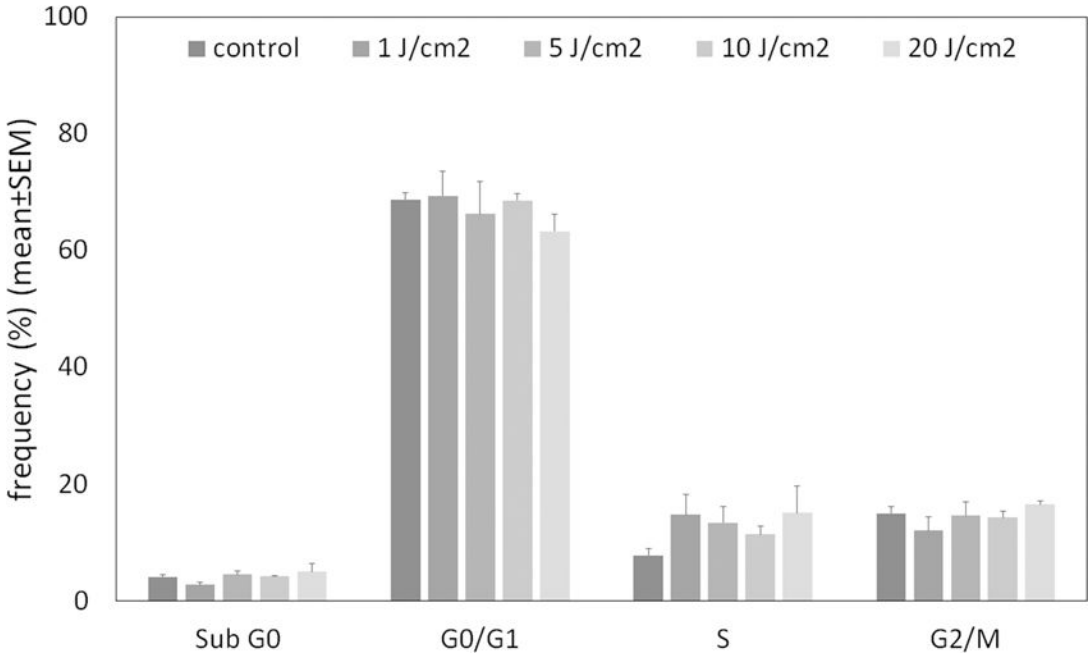


**Figure 8.**

Cell cycle distribution of HeLa cell following 685 nm PBM at 0 (control), 1, 5, 10, and 20 J/cm$^2$ energy densities. The data are shown as mean ± SEM for at least three independent experiments. Statistical analysis between the groups was determined by ANOVA; *P < 0.05, compared with non-irradiated cells.

## Table 1

Percentage of cells surviving after X-ray radiation in HeLa cell pre-exposed to 685 nm PBM according to clonogenic survival assay.

| Ionizing radiation dose | PBM energy density (J/cm$^2$) | | | |
|---|---|---|---|---|
| | 0 | 5 | 10 | 20 |
| 0 Gy | 100±0.8 | 99.9±0.04 | 99.7±0.2 | 99.9±0.01 |
| 2 Gy | 56.9±10.5 | 38.2±23.5 | 43.4±14 | 32.4±10.6 |
| 4 Gy | 24.8±2.2 | 20.1±2.4 | 19.3±2.1 | 12.5±2 * |
| 6 Gy | 4.2±1.6 | 4.1±2.8 | 3.1±1.3 | 1.7±0.7 * |

The data are shown as mean ± SEM for at least three independent experiments. Statistical analysis between the groups was determined by ANOVA;

* $P < 0.05$, compared with non-pre-exposed cells to PBM.